Publisher: GSA
Journal: GEOL: Geology
DOI:10.1130/G45235.1

Fe-rich ferropericlase and magnesiowüstite inclusions reflecting diamond formation rather than ambient mantle

Paolo Nimis[1], Fabrizio Nestola[1], Mariangela Schiazza[1*], Riccardo Reali[2], Giovanna Agrosì[3], Daniela Mele[3], Gioacchino Tempesta[3], Daniel Howell[1,4], Mark T. Hutchison[5], and Richard Spiess[1]

[1]Dipartimento di Geoscienze, Università di Padova, via G. Gradenigo 6, 35131 Padova, Italy

[2]Unité Matériaux et Transformations, Université Lille1, 59655 Villeneuve d'Ascq, France

[3]Dipartimento di Scienze della Terra e Geoambientali, Università degli Studi di Bari Aldo Moro, Via Orabona 4, 70125 Bari, Italy

[4]Department of Earth Sciences, University of Bristol, Bristol, BS8 1RJ, UK

[5]Trigon GeoServices Ltd., Las Vegas, Nevada 89146, USA

*Current address: Dipartimento di Scienze Psicologiche, della Salute e del Territorio DiSPuTer, Università G. D'Annunzio di Chieti-Pescara, 66100 Chieti, Italy

ABSTRACT

At the core of many Earth-scale processes is the question of what the deep mantle is made of. The only direct samples from such extreme depths are diamonds and their inclusions. It is often assumed that these inclusions reflect ambient mantle or are syngenetic with diamond, but these assumptions are rarely tested. We have studied inclusion–host growth relationships in two potentially superdeep diamonds from Juina

Publisher: GSA
Journal: GEOL: Geology
DOI:10.1130/G45235.1

(Brazil) containing nine inclusions of Fe-rich (X_{Fe} ≈0.33 to ≥0.64) ferropericlase–magnesiowüstite (FM) by X-ray diffractometry, X-ray tomography, cathodoluminescence, electron backscatter diffraction and electron microprobe analysis. The inclusions share a common [112] zone axis with their diamonds and have their major crystallographic axes within 3–8° of those of their hosts. This suggests a specific crystallographic orientation relationship (COR), resulting from interfacial energy minimization, disturbed by minor post-entrapment rotation around [112] due to plastic deformation. The observed COR and the relationships between inclusions and diamond growth zones imply that FM nucleated during the growth history of the diamond. Therefore, these inclusions may not provide direct information on the ambient mantle prior to diamond formation. Consequently, a 'non-pyrolitic' composition of the lower mantle is not required to explain the occurrence of Fe-rich FM inclusions in diamonds. By identifying examples of mineral inclusions which reflect the local environment of diamond formation and not ambient mantle, we provide both a cautionary tale and a means to test diamond/inclusion time relationships for proper application of inclusion studies to whole-mantle questions.

INTRODUCTION

Diamonds found in kimberlites and lamproites are our deepest samples of Earth's interior. Most diamonds come from deep lithospheric roots beneath cratons, but some rare diamonds are believed to have formed at sublithospheric levels, possibly as deep as the core/mantle boundary (see reviews in Stachel et al., 2005; Harte, 2010; Kaminsky, 2012). Ferropericlase–magnesiowüstite (Mg,Fe)O (hereafter FM) is the most common mineral contained in diamonds of interpreted lower-mantle origin and its composition has

Publisher: GSA
Journal: GEOL: Geology
DOI:10.1130/G45235.1

been recently used to estimate oxygen fugacity in the lower mantle (Otsuka et al., 2013; Kaminsky et al., 2015). This is notwithstanding the fact that FM also participates in mineral parageneses straddling the upper mantle/lower mantle boundary (Hutchison et al., 2001), the relative abundance of FM inclusions is higher than predicted by experiments on 'pyrolite' at lower-mantle conditions (48%–63% versus 16%–20%; e.g., Irifune, 1994; Fei and Bertka, 1999; Wood, 2000; Kaminsky, 2012), and their composition is more variable and often more Fe-rich than expected for FM in the lower mantle [$Fe/(Mg + Fe)_{mol} = X_{Fe}$ = 0.10–0.64 versus 0.10–0.27; e.g., Kesson and Fitz Gerald, 1992; Wood, 2000; Lee et al., 2004]. Fe-rich compositions characterize a significant proportion (ca. 46.5%) of FM inclusions in Brazilian stones (Kaminsky, 2012).

Several hypotheses have been put forward to explain the existence of Fe-rich FM. These hypotheses can be grouped into two categories: (i) the Fe-rich composition is considered to reflect a 'non-pyrolitic' composition of the ambient lower mantle, samples of which were captured by the growing diamonds (Harte et al., 1999; Kaminsky, 2012; Ryabchikov and Kaminsky, 2013; Kaminsky and Lin, 2017); (ii) formation of Fe-rich FM *and* diamond is ascribed to reactions involving carbonate melts or minerals in the lower mantle (Liu, 2002; Litvin, 2014) or in the deep upper mantle and transition zone (Thomson et al., 2016). This contrast of views is partly justified by the fact that the traditional criterion used to identify syngenetic inclusions (i.e., a diamond-imposed shape) has proven unreliable (Nestola et al., 2014). Therefore, there is still uncertainty as to whether Fe-rich FM inclusions represent accidentally encapsulated portions of an anomalous ambient mantle or a product of reactions occurring during the growth history

Publisher: GSA
Journal: GEOL: Geology
DOI:10.1130/G45235.1

of diamond. As diamonds and their mineral inclusions are such important windows on mantle composition and processes it is critical to test these conflicting hypotheses. This may have profound implications on our interpretation of the mechanisms of formation of sublithospheric diamonds and on the significance of petrological and geochemical data extracted from their inclusions (e.g., Shirey et al., 2013; Thomson et al., 2014, 2016).

Here we investigate the growth relationships of nine Fe-rich (X_{Fe} = 0.33 to ≥0.64) FM inclusions in two diamonds from the notable alluvial deposits of tributaries of the Rio Aripuanã, Juina district, Brazil (e.g., Hutchison et al., 2004; see detailed provenance data in the GSA Data Repository[1]). We will show that our Fe-rich FM formed by direct segregation from a fluid or melt or from fluid/melt-assisted dissolution-precipitation during the growth history of their diamond hosts. Hence, the entrapped FM inclusions should not be considered as representative samples of the ambient mantle in which the diamond-forming processes took place.

SAMPLE MATERIAL AND ANALYTICAL METHODS

The diamonds studied in the present work (BZ270 and JUc4) appeared as irregular, brown-colored stones, with maximum dimensions of 7 and 3 mm, respectively. Sample preparation and analyses were conducted in such a way as to preserve as much of the samples as possible for future investigations. The stones were polished on two opposite sides to obtain small windows that allowed visual recognition of most of their inclusions. The FM inclusions showed a faceted to subround shape, sometimes with concave angles, and maximum dimensions of a few 10s to 500 μm (Fig. 1A,B). The largest inclusions in diamond BZ270 exhibited stepped surfaces on some of the faces (Fig. 1B). Decompression cracks were observed around most of the inclusions. Micro-

Publisher: GSA
Journal: GEOL: Geology
DOI:10.1130/G45235.1

computed X-ray tomography (μ-CT) of diamond BZ270 showed the presence of numerous additional inclusions, which have a size up to a few μm and are distributed along a set of interconnected {111} diamond planes (Fig. 1C and supplementary video in the Data Repository).

Previous investigation by X-ray diffraction topography (XRDT) showed that both samples are affected by plastic deformation (Agrosì et al., 2017). BZ270 is more strongly deformed and consists of an aggregate of different 'grains', which are misoriented by at least a few seconds of arc, whereas JUc4 appears to be a single grain. Micro Fourier-transform infrared spectroscopy (μFTIR) (Agrosì et al., 2017) showed that BZ270 was predominantly Type IIa (i.e., nitrogen below detection of ~10 ppm; Fig. 2D). The μFTIR of a portion of JUc4 suggested the presence of a more N-rich core (270 ppm N, 100% IaB, no platelets) and decreasing N content toward the rim (~40 ppm, 100% IaB, no platelets) (Fig. 1E).

Both samples were studied by single-crystal X-ray diffraction (XRD) to determine the approximate chemical compositions of the FM inclusions and their crystallographic orientation relationships (CORs) with the diamonds. Diamond BZ270 was then further polished to expose some of the large and small inclusions and investigated by cathodoluminescence (CL) and electron backscatter diffraction (EBSD). Electron microprobe analysis (EMPA) was performed on the exposed inclusions (Table DR1). Additional details on analytical methods are given in the Data Repository[1].

RESULTS

The analyzed FM inclusions have their major crystallographic axes within 3–8° of those of the host diamonds (Fig. 2, Table DR2). Despite this minor misorientation, the

Publisher: GSA
Journal: GEOL: Geology
DOI:10.1130/G45235.1

116 angular mismatch between the [112] axes of the inclusions and those of the diamonds is
117 remarkably small (< 2°), i.e., within the uncertainty of the measurements (cf. Nestola et
118 al., 2014), and the inclusions appear to be mutually rotated around the [112] axis of their
119 host (Fig. 2).

120 The CL images of sample BZ270 show a complex growth–resorption pattern,
121 disturbed by plastic deformation (Fig. 1F–H), as commonly observed in sublithospheric
122 diamonds (Shirey et al., 2013). EBSD data are consistent with the activation of
123 {111}<011> slip systems (Fig. DR3 in the GSA Data Repository[1]), a mechanism
124 observed in several natural and experimentally deformed diamonds (Howell et al., 2012).
125 Domains characterized by slightly different lattice orientations (up to 3.5°) are observed,
126 which show no special relationship with the distribution of the inclusions (Fig. DR3).
127 Polishing of diamond BZ270 allowed us to uncover two of the FM inclusions and three
128 of the aligned, μm-sized inclusions. The FM inclusions sit on distinct diamond growth
129 zones (Fig. 1G). The analyzed μm-sized inclusions have a composition corresponding to
130 Ni-poor pyrrhotite (Table DR1), within the compositional range reported for other Juina
131 diamonds (Hutchison, 1997), and are located at the boundary between two more external
132 CL growth bands (Fig. 1H).

133 The compositions of the FM inclusions indicate an X_{Fe} range of ca. 0.33 to ≥0.64
134 (Table 1). Because high-quality XRD and EMPA data could be obtained only on some of
135 the inclusions, some X_{Fe} data have large uncertainties, but they are sufficient to establish
136 a relatively Fe-rich composition for all studied inclusions. Data for sample JUc4 suggest
137 a progressive X_{Fe} increase in inclusions sitting outside the N-rich diamond core. The
138 moderate NiO (0.4 wt. %) and very low Na_2O (<0.06 wt. %) contents measured on

Publisher: GSA
Journal: GEOL: Geology
DOI:10.1130/G45235.1

exposed inclusions n. 4 and 5 in diamond BZ270 (Table DR1) are in line with those reported for FM inclusions of similar X_{Fe} in worldwide diamonds (Thomson et al., 2016).

DISCUSSION AND CONCLUSIONS

Data for multiple inclusions in two stones indicate a non-random COR between FM and diamond (Fig. 2; Table DR2). The nearly parallel orientation of FM's and diamond's crystal lattices suggests an original *specific COR* (cf. Griffiths et al., 2016). Post-entrapment plastic deformation in the diamond along {111}<011> slip systems (Fig. DR3), with consequent slight rotation of the inclusions around the normal [112] axis (Fig. 2), may well account for the small observed angular mismatch. Consistently, this particular type of rotational COR was not observed in inclusions from less deformed lithospheric diamonds (Nestola et al., 2014; Milani et al., 2016).

A specific COR may result from interface energy minimization (i) on precipitation from a fluid/melt, during mutual growth or when one of the two minerals provides a substrate for nucleation of the other (e.g., Mutaftschiev, 2001), (ii) on static recrystallization, when the small effect of interface energies is not swamped in magnitude by that of imposed stress (Wheeler et al., 2001), or (iii) on fluid/melt-assisted recrystallization, when dissolution–precipitation and epitaxial nucleation of new grains occur (Putnis and Austrheim, 2010). Scenario (ii) is highly unlikely in our case, given the high-stress environment in which our diamonds have formed. Scenario (iii) is most likely accompanied by chemical resetting and in fact, with increasing solid–fluid disequilibrium, may grade into scenario (i). Note that the distinction between 'fluid' and 'melt' tends to vanish with increasing pressure and may not exist under sub-lithospheric conditions (Luth, 2014). Mechanical interactions between euhedral crystals can also

Publisher: GSA
Journal: GEOL: Geology
DOI:10.1130/G45235.1

potentially lead to non-random COR (Wheeler et al., 2001). However, in this case only one inclusion crystallographic direction, normal to the contact face, is fixed to the host. Therefore, a statistical rotational relationship (cf. Griffiths et al., 2016) rather than a strongly clustered orientation would be expected. Note that {112} faces are not found in periclase-group minerals and are uncommon in diamond (Goldschmidt, 1916; Gaines et al., 1997); therefore, they are unlikely to have played any role in determining the minor rotational component in the observed COR (Fig. 2).

The distribution of the FM inclusions relative to diamond growth zones (Fig. 1G,H) and N zoning (Fig. 1D,E) indicates that at least some of them are sitting well away from the diamond growth centers and, thus, cannot have acted as seeds for diamond nucleation (cf. the 'central inclusions' in Bulanova, 1995, and Bulanova et al., 1998). Moreover, none of the FM inclusions are located on healed cracks or subgrain boundaries (Fig. 1G,H and DR3), which excludes that the inclusions were formed or modified after diamond formation. Therefore, either diamond and FM precipitated from the same parent medium, i.e., they are syngenetic, or FM nucleated epitaxially on diamond and was later incorporated during a further episode of diamond growth. Whatever the nucleation mechanism (dissolution–precipitation or precipitation as a new mineral), our Fe-rich FM inclusions may not represent accidentally encapsulated portions of the ambient mantle, but rather the product of reactions occurring during the growth history of diamond. A similar conclusion can be drawn for the tiny pyrrhotite inclusions in diamond BZ270, sitting at the boundary between two diamond growth zones (Fig. 1C,H). Their low-Cr, low-Ni composition (Table DR1) suggests an 'eclogitic' or melt-rich environment.

Publisher: GSA
Journal: GEOL: Geology
DOI:10.1130/G45235.1

FM compositions in diamond JUc4 (X_{Fe} = 0.43 to ≥0.64) show no overlap with the range for FM in association with former bridgmanite (X_{Fe} = 0.10–0.36, median = 0.17, N = 19; Hutchison, 1997; Stachel et al., 2000; Davies et al., 2004; Hayman et al., 2005; Tappert et al., 2009; Zedgenizov et al., 2014), and FM compositions in diamond BZ270 are tightly clustered at its Fe-rich end. This suggests that the processes recorded in our diamonds may not be typical of the lower mantle. Indeed, experiments by Thomson et al. (2016) suggest that precipitation of variously Fe-enriched FM and diamond may occur by reaction of slab-derived carbonatite melt with mantle rocks, at varying melt/rock ratios, in the deep upper mantle and transition zone. This scenario is fully compatible with our observations and provides a plausible mechanism for formation of our FM-bearing diamonds at depths shallower than the lower mantle under increasing melt/rock ratio.

Our interpretation of Fe-rich FM inclusions as a product of reactions occurring during the growth history of diamond may potentially apply to other FM inclusions for which evidence of pre-diamond formation is lacking. Therefore, using FM inclusions to provide direct information on the composition of the ambient mantle and, particularly, of the lower mantle is unwarranted. Specifically, a 'non-pyrolitic' composition of the lower mantle is not required to explain the occurrence of Fe-rich FM inclusions in diamonds. By identifying examples of mineral inclusions which reflect local growth conditions rather than ambient mantle we emphasize the importance of, and provide a means for testing host/inclusion time relationships in strongly deformed diamonds.

ACKNOWLEDGMENTS

Publisher: GSA
Journal: GEOL: Geology
DOI:10.1130/G45235.1

Material for the present study was supplied by MTH. This research was supported by the Alfred P. Sloan Foundation's Deep Carbon Observatory (DMGC-project), ERC Starting Grant INDIMEDEA to FN (agreement n. 307322), CPDA 122324/12 and FACCPRAT12 grants (University of Padova) and National Project PONa3_00369 "SISTEMA" (University of Bari). Constructive reviews by F. Kaminsky and two anonymous reviewers helped us improve the manuscript.

REFERENCES CITED

Agrosì, G., Tempesta, G., Della Ventura, G., Cestelli Guidi, M., Hutchison, M., Nimis, P., and Nestola, F., 2017, Non-destructive in situ study of plastic deformations in diamonds: X-ray diffraction topography and μFTIR mapping of two super deep diamond crystals from São Luiz (Juina, Brazil): Crystals, v. 7, p. 233, doi:https://doi.org/10.3390/cryst7080233.

Angel, R., Milani, S., Alvaro, M., and Nestola, F., 2015, OrientXplot: a program to analyse and display relative crystal orientations: Journal of Applied Crystallography, v. 48, p. 1330–1334, doi:https://doi.org/10.1107/S160057671501167X.

Bulanova, G.P., 1995, The formation of diamond: Journal of Geochemical Exploration, v. 53, p. 1–23, https://doi.org/10.1016/0375-6742(94)00016-5.

Bulanova, G.P., Griffin, W.L., and Ryan, C.G., 1998, Nucleation environment of diamonds from Yakutian kimberlites: Mineralogical Magazine, v. 62, p. 409–419, doi:https://doi.org/10.1180/002646198547675.

Davies, R.M., Griffin, W.L., O'Reilly, S.Y., and Doyle, B.J., 2004, Mineral inclusions and geochemical characteristics of microdiamonds from the DO27, A154, A21,

A418, DO18, DD17 and Ranch Lake kimberlites at Lac de Gras, Slave Craton, Canada: Lithos, v. 77, p. 39–55, doi:https://doi.org/10.1016/j.lithos.2004.04.016.

Fei, Y., and Bertka, C.M., 1999, Phase transitions in the Earth's mantle and mantle mineralogy, *in* Fei, Y., et al., eds., Mantle Petrology: Field Observations and High Pressure Experimentation; a Tribute to Francis R. (Joe) Boyd: Geochemical Society London Special Publication 6, p. 189–207.

Gaines, R.V., Catherine, H., Skinner, W., Foord, E.E., Mason, B., and Rosenzweig, A., 1997, Dana's new mineralogy: the system of mineralogy of James Dwight Dana and Edward Salisbury Dana, Eighth Edition: New York, John Wiley & Sons, Inc., 1819 p.

Goldschmidt, V., 1916, Atlas der Krystallformen: Heidelberg, Germany, Carl Winters Universitatsbuchhandlung, 144 p.

Griffiths, T.A., Habler, G., and Abart, R., 2016, Crystallographic orientation relationships in host–inclusion systems: New insights from large EBSD data sets: The American Mineralogist, v. 101, p. 690–705, doi:https://doi.org/10.2138/am-2016-5442.

Harte, B., Harris, J.W., Hutchison, M.T., Watt, G.R., and Wilding, M.C., 1999, Lower mantle mineral associations in diamonds from Sao Luiz, Brazil, *in* Fei, Y., et al., eds., Mantle Petrology: Field Observations and High Pressure Experimentation; a tribute to Francis R. (Joe) Boyd: Geochemical Society, London, Special Publication 6, p. 125–153.

Harte, B., 2010, Diamond formation in the deep mantle: the record of mineral inclusions and their distribution in relation to mantle dehydration zones: Mineralogical Magazine, v. 74, p. 189–215, doi:https://doi.org/10.1180/minmag.2010.074.2.189.

Hayman, P.C., Kopylova, M.G., and Kaminsky, F.V., 2005, Lower mantle diamonds from Rio Soriso (Juina, Brazil): Contributions to Mineralogy and Petrology, v. 149, p. 430–445, doi:https://doi.org/10.1007/s00410-005-0657-8.

Howell, D., Piazolo, S., Dobson, D.P., Wood, I.G., Jones, A.P., Walte, N., Frost, D.J., Fisher, D., and Griffin, W.L., 2012, Quantitative characterization of plastic deformation of single diamond crystals: A high pressure high temperature (HPHT) experimental deformation study combined with electron backscatter diffraction (EBSD): Diamond and Related Materials, v. 30, p. 20–30, doi:https://doi.org/10.1016/j.diamond.2012.09.003.

Hutchison, M.T., 1997, Constitution of the deep transition zone and lower mantle shown by diamonds and their inclusions [Ph.D. thesis]: University of Edinburgh, 660 p. and CDRom.

Hutchison, M.T., Hursthouse, M.B., and Light, M.E., 2001, Mineral inclusions in diamonds: associations and chemical distinctions around the 670-km discontinuity: Contributions to Mineralogy and Petrology, v. 142, p. 119–126, doi:https://doi.org/10.1007/s004100100279.

Hutchison, M.T., Nixon, P.H., and Harley, S.L., 2004, Corundum inclusions in diamonds - discriminatory criteria and a corundum compositional database: Lithos, v. 77, p. 273–286, doi:https://doi.org/10.1016/j.lithos.2004.04.006.

Irifune, T., 1994, Absence of an aluminous phase in the upper part of the Earth's lower mantle: Nature, v. 370, p. 131–133, https://doi.org/10.1038/370131a0.

Kaminsky, F.V., 2012, Mineralogy of the lower mantle: A review of 'super-deep' mineral inclusions in diamond: Earth-Science Reviews, v. 110, p. 127–147, doi:https://doi.org/10.1016/j.earscirev.2011.10.005.

Kaminsky, F.V., and Lin, J.-F., 2017, Iron partitioning in natural lower-mantle minerals: Toward a chemically heterogeneous lower mantle: The American Mineralogist, v. 102, p. 824–832, doi:https://doi.org/10.2138/am-2017-5949.

Kaminsky, F.V., Ryabchikov, I.D., McCammon, C.A., Longo, M., Abakumov, A.M., Turner, S., and Heidari, H., 2015, Oxidation potential in the Earth's lower mantle as recorded by ferropericlase inclusions in diamond: Earth and Planetary Science Letters, v. 417, p. 49–56, doi:https://doi.org/10.1016/j.epsl.2015.02.029.

Kesson, S.E., and Fitz Gerald, J.D., 1992, Partitioning of MgO, FeO, NiO, MnO and Cr_2O_3 between magnesian silicate perovskite and magnesiowüstite: implications for the origin of inclusions in diamond and the composition of the lower mantle: Earth and Planetary Science Letters, v. 111, p. 229–240, https://doi.org/10.1016/0012-821X(92)90181-T.

Lee, K.K.M., O'Neill, B., Panero, W.R., Shim, S.H., Benedetti, L.R., and Jeanloz, R., 2004, Equations of state of the high-pressure phases of a natural peridotite and implications for the Earth's lower mantle: Earth and Planetary Science Letters, v. 223, p. 381–393, doi:https://doi.org/10.1016/j.epsl.2004.04.033.

Litvin, Y.A., 2014, The stishovite paradox in the genesis of superdeep diamonds: Doklady Earth Sciences, v. 455, p. 274–278, doi:https://doi.org/10.1134/S1028334X14030064.

294 Liu, L., 2002, An alternative interpretation of lower mantle mineral associations in
295 diamonds: Contributions to Mineralogy and Petrology, v. 144, p. 16–21,
296 doi:https://doi.org/10.1007/s00410-002-0389-y.
297 Luth, R.W., 2014, 3.9 — Volatiles in Earth's mantle, *in* Holland, H.D., and Turekian,
298 K.K., eds., Treatise on Geochemistry: Elsevier Oxford, p. 355–391, doi:
299 https://doi.org/10.1016/B978-0-08-095975-7.00207-2.
300 Milani, S., Nestola, F., Angel, R.J., Nimis, P., and Harris, J.W., 2016, Crystallographic
301 orientations of olivine inclusions in diamonds: Lithos, v. 265, p. 312–316,
302 https://doi.org/10.1016/j.lithos.2016.06.010.
303 Mutaftschiev, B., 2001, The Atomistic Nature of Crystal Growth: Springer-Verlag Berlin
304 Heidelberg New York, v. 43, 368 p.
305 Nestola, F., Nimis, P., Angel, R.J., Milani, S., Bruno, M., Prencipe, M., and Harris, J.W.,
306 2014, Olivine with diamond-imposed morphology included in diamonds. Syngenesis
307 or protogenesis?: International Geology Review, v. 56, p. 1658–1667,
308 doi:https://doi.org/10.1080/00206814.2014.956153.
309 Otsuka, K., Longo, M., McCammon, C.A., and Karato, S.-i., 2013, Ferric iron content of
310 ferropericlase as a function of composition, oxygen fugacity, temperature and
311 pressure: implications for redox conditions during diamond formation in the lower
312 mantle: Earth and Planetary Science Letters, v. 365, p. 7–16,
313 https://doi.org/10.1016/j.epsl.2012.11.030.
314 Putnis, A., and Austrheim, H., 2010, Fluid-induced processes: Metasomatism and
315 metamorphism: Geofluids, v. 10, p. 254–269, doi:10.1111/j.1468-
316 8123.2010.00285.x.

317 Ryabchikov, I.D., and Kaminsky, F.V., 2013, The composition of the lower mantle:
318 Evidence from mineral inclusions in diamonds: Doklady Earth Sciences, v. 453,
319 p. 1246–1249, https://doi.org/10.1134/S1028334X13120155.
320 Shirey, S.B., Cartigny, P., Frost, D.J., Keshav, S., Nestola, F., Nimis, P., Pearson, D.G.,
321 Sobolev, N.V., and Walter, M.J., 2013, Diamonds and the geology of mantle carbon,
322 *in* Hazen, R.M., et al., eds., Carbon in Earth: Reviews in Mineralogy and
323 Geochemistry, v. 75, p. 355–421, doi:https://doi.org/10.2138/rmg.2013.75.12.
324 Stachel, T., Brey, G.P., and Harris, J.W., 2005, Inclusions in sublithospheric diamonds:
325 glimpses of deep Earth: Elements, v. 1, p. 73–78,
326 doi:https://doi.org/10.2113/gselements.1.2.73.
327 Stachel, T., Harris, J.W., Brey, G.P., and Joswig, W., 2000, Kankan diamonds (Guinea)
328 II: lower mantle inclusion paragenesis: Contributions to Mineralogy and Petrology,
329 v. 140, p. 16–27, https://doi.org/10.1007/s004100000174.
330 Tappert, R., Foden, J., Stachel, T., Muehlenbachs, K., Tappert, M., and Wills, K., 2009,
331 Deep mantle diamonds from South Australia: A record of Pacific subduction at the
332 Gondwanan margin: Geology, v. 37, p. 43–46,
333 doi:https://doi.org/10.1130/G25055A.1.
334 Thomson, A.R., Kohn, S.C., Bulanova, G.P., Smith, C.B., Araujo, D., EIMF, and Walter,
335 M.J., 2014, Origin of sub-lithospheric diamonds from the Juina-5 kimberlite (Brazil):
336 constraints from carbon isotopes and inclusion compositions: Contributions to
337 Mineralogy and Petrology, v. 168, p. 1081, doi:https://doi.org/10.1007/s00410-014-
338 1081-8.

Thomson, A.R., Walter, M.J., Kohn, S.C., and Brooker, R.A., 2016, Slab melting as a barrier to deep carbon subduction: Nature, v. 529, p. 76–79, doi:https://doi.org/10.1038/nature16174.

Wheeler, J., Prior, D.J., Jiang, Z., Spiess, R., and Trimby, P.J., 2001, The petrological significance of misorientations between grains: Contributions to Mineralogy and Petrology, v. 141, p. 109–124, https://doi.org/10.1007/s004100000225.

Wood, B.J., 2000, Phase transformations and partitioning relations in peridotite under lower mantle conditions: Earth and Planetary Science Letters, v. 174, p. 341–354, doi:https://doi.org/10.1016/S0012-821X(99)00273-3.

Zedgenizov, D.A., Kagi, H., Shatsky, V.S., and Ragozin, A.L., 2014, Local variations of carbon isotope composition in diamonds from São-Luis (Brazil): evidence for heterogeneous carbon reservoir in sublithospheric mantle: Chemical Geology, v. 363, p. 114–124, https://doi.org/10.1016/j.chemgeo.2013.10.033.

Publisher: GSA
Journal: GEOL: Geology
DOI:10.1130/G45235.1

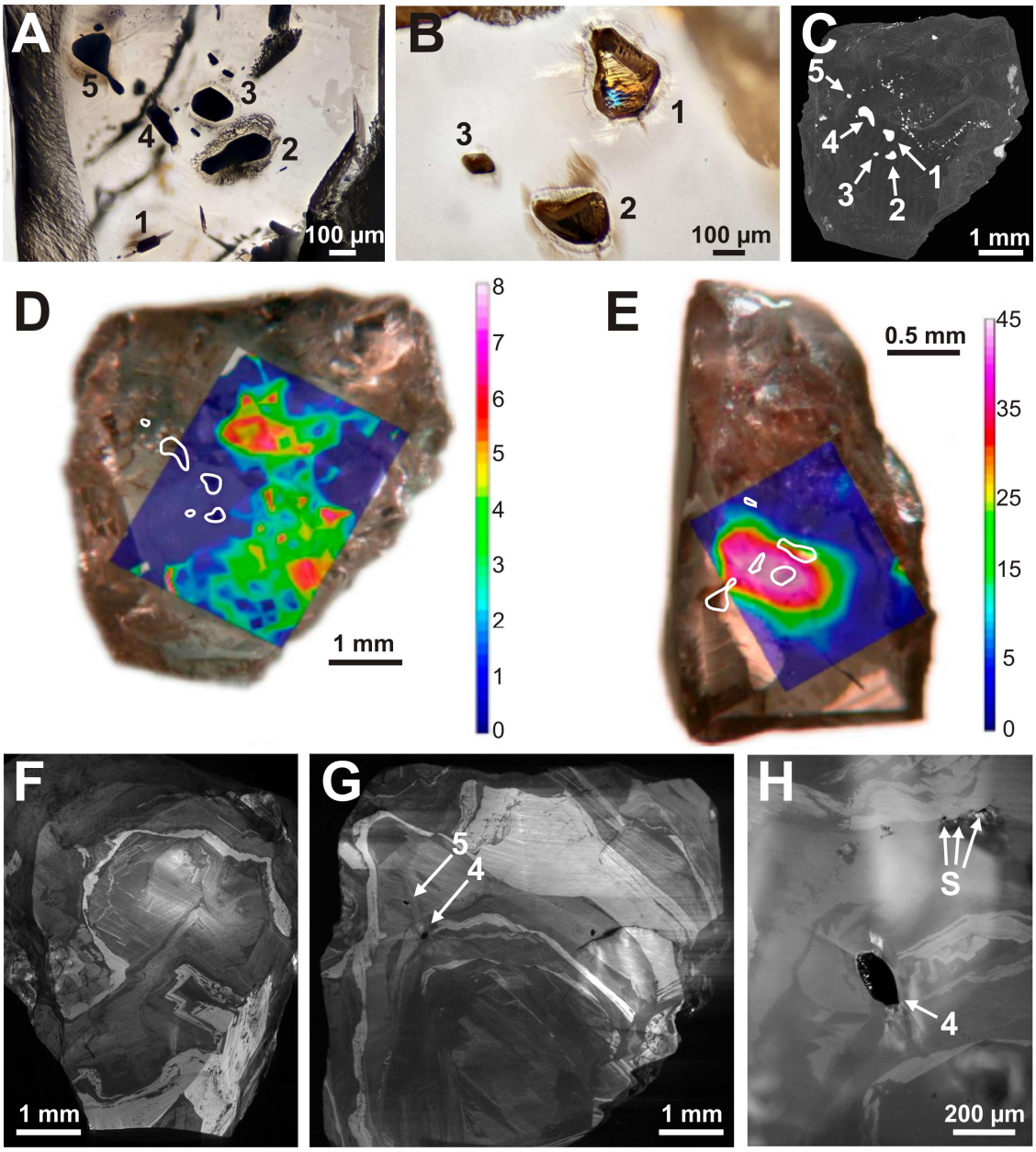

Figure 1. (A-B) Microphotographs of FM inclusions in polished diamonds JUc4 (A, transmitted light) and BZ270 (B, transmitted plus incident light); (C) µ-CT image of diamond BZ270, showing a cluster of FM inclusions (numbered) and a trail of tiny inclusions; (D) FTIR map of diamond BZ270; the color scale, from blue (zero intensity) to red/whitish (max intensity), is qualitative and given the low values is not necessarily

Publisher: GSA
Journal: GEOL: Geology
DOI:10.1130/G45235.1

related to N concentration; white outlines indicate projection of the FM inclusions (mod. after Agrosì et al., 2017); (E) same as in (D) for diamond JUc4, but here the color scale has been confirmed to correlate to N concentration (mod. after Agrosì et al., 2017); (F) CL image of diamond BZ270 after limited polishing; (G-H) CL images of reverse side of diamond BZ270 after different degrees of polishing, with exposed FM and sulfide (S) inclusions. Numbers in (A-C) and (G-H) as in Table 1.

Publisher: GSA
Journal: GEOL: Geology
DOI:10.1130/G45235.1

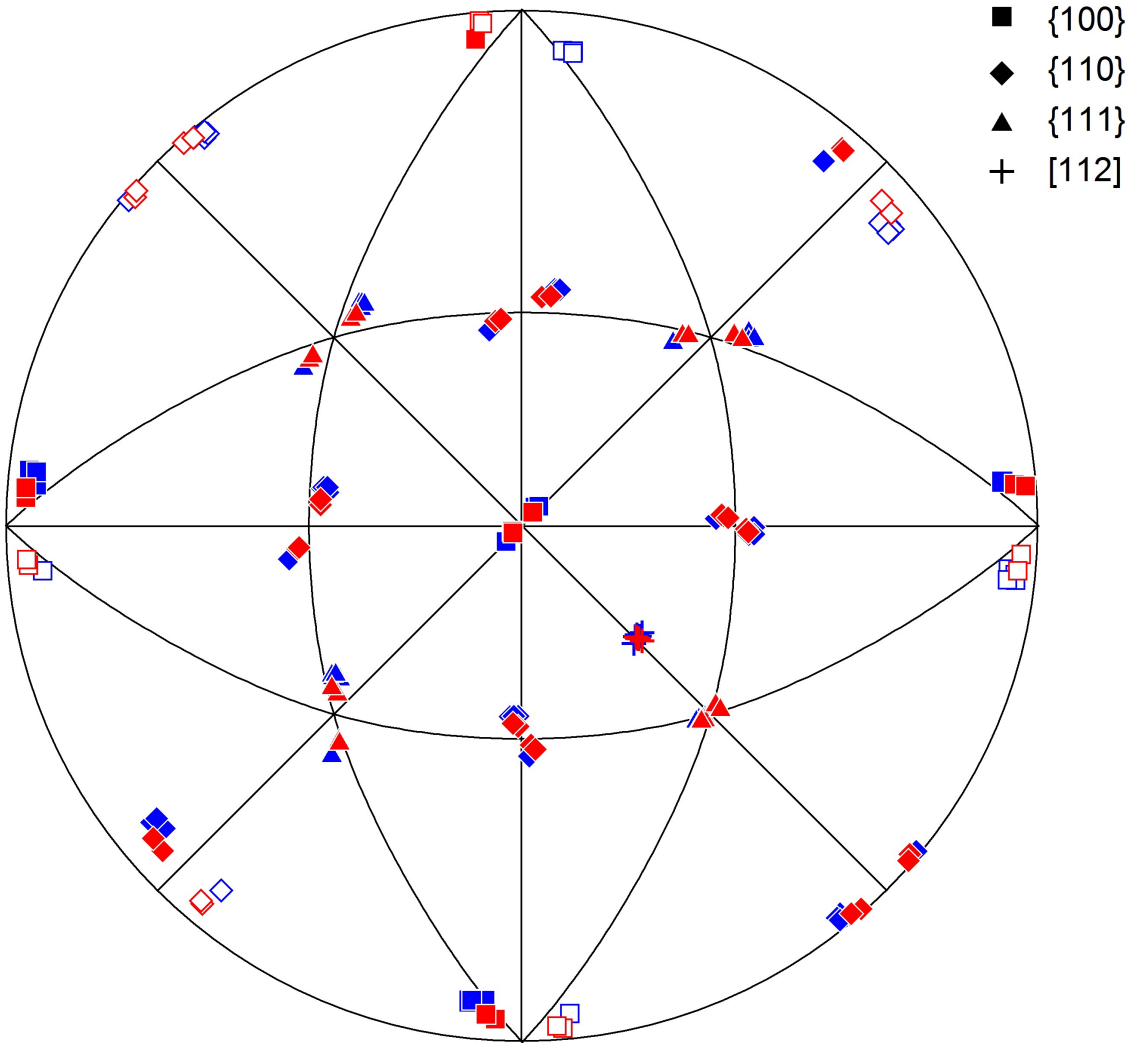

Figure 2. Crystallographic orientations of FM inclusions relative to their diamond hosts, plotted using the OrientXplot software (Angel et al., 2015). Open symbols plot in lower hemisphere. Blue symbols = BZ270; red symbols = JUc4.

1GSA Data Repository item 2018xxx, sample location and analytical methods and micro-computed X-ray tomography (μ-CT) of diamond BZ270 (video), is available online at http://www.geosociety.org/datarepository/2018/, or on request from editing@geosociety.org.

Publisher: GSA
Journal: GEOL: Geology
DOI:10.1130/G45235.1

TABLE 1. COMPOSITIONAL DATA FOR FM INCLUSIONS

Diamond	Inclusion	X_{Fe} (site occ.)*	X_{Fe} (*a* edge)†	X_{Fe} (EMPA)§
BZ270	1	0.31(2)	≥0.34(2)	–
	2	0.31(2)	≥0.35(2)	–
	3	–	≥0.35(5)	–
	4	–	0.34(2)	0.346(3)
	5	0.36(2)	0.35(2)	0.338(0)
JUc4	2	–	≥0.57(5)	–
	3	–	≥0.44(5)	–
	4	–	≥0.43(6)	–
	5	–	≥0.64(3)	–

Note: Numbers in parentheses are 1·σ uncertainties on the last digit. See the Data Repository[1] for details on evaluation of chemical compositions.

*Based on site occupancies after crystal structure refinement.

†Based on equation $X_{Fe} = 8.441 \cdot a$ (Å) – 35.553, valid for stoichiometric FM at room pressure; minimum values for unexposed inclusions analyzed in situ, which may be under residual pressure.

§Based on EMPA analysis of exposed inclusions (Table DR1).